Received: 14 February 2018 | Accepted: 18 June 2018

DOI: 10.1111/1365-2745.13033

RESEARCH ARTICLE

Journal of Ecology | BRITISH ECOLOGICAL SOCIETY

Divergent temporal trends of net biomass change in western Canadian boreal forests

Yong Luo[1,2] | Han Y. H. Chen[1,3] | Eliot J. B. McIntire[2,4] | David W. Andison[2,5]

[1]Faculty of Natural Resources Management, Lakehead University, Thunder Bay, ON, Canada

[2]Faculty of Forestry, University of British Columbia, Vancouver, BC, Canada

[3]Key Laboratory of Subtropical Mountain Ecology, College of Geographical Sciences, Fujain Normal University, Fujian, China

[4]Canadian Forest Service, Natural Resources Canada, Pacific Forestry Centre, Victoria, BC, Canada

[5]Bandaloop Landscape-Ecosystem Services, Nelson, BC, Canada

Correspondence
Han Y. H. Chen, Faculty of Natural Resources Management, Lakehead University, 955 Oliver Road, Thunder Bay, ON P7B 5E1, Canada.
Email: hchen1@lakeheadu.ca

Funding information
Natural Sciences and Engineering Research Council of Canada, Grant/Award Number: RGPIN-2014-04181 and STPGP 506284

Handling Editor: Frank Gilliam

Abstract

1. Forests play a strong role in the global carbon cycle by absorbing atmospheric carbon dioxide through increasing forest biomass. Understanding temporal trends of forest net above-ground biomass change (ΔAGB) can help infer how forest carbon sequestration responds to ongoing climate changes. Despite wide spatial variation in the long-term average of climate moisture availability ($CMI_{average}$) across forest ecosystems, temporal trends of ΔAGB associated with $CMI_{average}$ remain unclear.
2. We tested the hypothesis that the negative impacts of climate change on ΔAGB would decrease with $CMI_{average}$ using the data from permanent sample plots, monitored from 1958 to 2011, with stand ages varying from 17 to 210 years, in western boreal forests of Canada.
3. We found that ΔAGB on average increased with $CMI_{average}$. Temporally, ΔAGB declined sharply between 1958 and 2011 in plots with low $CMI_{average}$ owing to increased biomass loss from mortality accompanied by little growth gain, whereas ΔAGB changed little in plots with high $CMI_{average}$. The temporal decrease of ΔAGB in drier areas was attributable to its negative responses to warming-induced temporal decreases in climate moisture availability.
4. *Synthesis*. Our results indicate that large-scale changes in forest carbon functioning associated with climate change depend on the long-term average of climate moisture availability. Our finding suggests a possible retreat of boreal biome at the drier distribution limits with predicted declines in water availability in the 21st century.

KEYWORDS
boreal forests, climate change, elevated atmospheric CO_2, global change ecology, global warming, growth, mortality, net above-ground biomass change, spatial climate moisture availability

1 | INTRODUCTION

Forests are our most important repositories of terrestrial biodiversity and provide a wide range of valuable goods and services (Food and Agriculture Organization of the United Nations, 2015). The boreal forest alone stores nearly half of the global forest carbon, and its continued role as part of the global carbon cycle is a critical element of sustainability (Dixon et al., 1994; Pan et al., 2011). Temporal trends of net above-ground biomass change (ΔAGB) of established forests help infer how forest carbon sequestration responds to recent climate changes (Brienen et al., 2015; Chen, Luo, Reich, Searle, & Biswas, 2016; Ma et al., 2012; Pan et al., 2011). The

impact of climate change on ΔAGB in the boreal could be dependent on the balance between the positive effects of CO_2 fertilization and the negative effects of decreased water availability (Bradshaw & Warkentin, 2015; Liu et al., 2015; Ma et al., 2012). Recent studies suggest that the net effect of climate change on boreal biomass dynamics may reflect the spatial variation in water availability (D'Orangeville et al., 2016; Girardin, Hogg, et al., 2016). However, the degree to which spatial climate moisture availability influences climate change-associated temporal changes in forest biomass has not been explicitly examined. Such knowledge is critical to our understanding and prediction of the potential impacts of climate change on biomass accumulation in global forests, where both long-term averages and temporal trends of climate moisture availability vary spatially (Dai, 2013).

The temporal dynamics of forest biomass may depend strongly on long-term water availability. In dry climatic systems, forests are under water stress and have high mortality accompanied by slow growth rates (Allen, Breshears, & McDowell, 2015; Anderegg et al., 2015; Hogg, Michaelian, Hook, & Undershultz, 2017). Further climate change-induced declines in water availability may exceed the coping mechanisms of forests (Allen et al., 2015; Wang et al., 2014). Based on the limiting resource theory (Bloom, Chapin, & Mooney, 1985), forests under water stress may not benefit from these positive climate change drivers, even though rising CO_2, warming and extended growing seasons may be beneficial to forest growth (Brienen et al., 2015; Chen et al., 2018; D'Orangeville et al., 2016; Hogg et al., 2017; Pretzsch, Biber, Schutze, Uhl, & Rotzer, 2014; Wang et al., 2014).

Here, we sought to examine the spatiotemporal patterns in ΔAGB, and its two components, growth (biomass increment of surviving trees and in-growth by new recruitment trees) and mortality (biomass loss from dead trees), along with a gradient of the long-term average of climate moisture availability ($CMI_{average}$) in the western boreal forest of Canada. We also examined the sensitivity of ΔAGB, growth and mortality to regional climate change drivers such as rising atmospheric CO_2, warming and decreasing climate moisture availability. We analysed data from 871 permanent sampling plots (PSPs; Figure 1) that had repeated measurements between 1958 and 2011 (Figure 1 and Supporting Information Figure S1). These plots span a wide range of water availability over both space and time, as indicated by average and temporal trends of annual climate moisture index between 1958 and 2011 (Figure 1 and Supporting Information Table S1). We used a multivariate mixed effect model to examine the simultaneous effects of stand age and calendar year on ΔAGB, growth and mortality because of the dependency of ΔAGB on growth and mortality (Supporting Information Figure S2a and details in Section).

2 | MATERIALS AND METHODS

2.1 | Study area and the forest inventory data

Our study area in Alberta and Saskatchewan of Canada (49.01–59.73 N; −101.74 to −119.66 W; Figure 1) ranged in elevation from 260 to 2073 m above sea level. Between 1950 and 2009, mean annual temperature varied from −2.38°C to 4.08°C and mean annual precipitation from 365 to 1184 mm. The major stand-replacing natural disturbance in this area is wildfire, with return intervals varying from 15 to 90 years (Larsen, 1997; Weir, Johnson, & Miyanishi, 2000). A total of 2911 permanent sampling plots were established by the Alberta and Saskatchewan governments to monitor forest growth using stratified random sampling, mostly during the 1960s and 1970s. The plots, which varied in size from 405 to 8092 m^2, were established in stands (>1 ha in area) that were visually homogeneous in structure and composition. The plots were located at least 100 m from any openings to minimize edge effects.

Similar to Chen et al. (2016), the dataset was selected based on four criteria: (a) forests with known ages originated from wildfire and were not managed; (b) plots had been monitored for ≥10 years and ≥3 censuses and; (c) all trees within sample plots including recruitment trees, whose diameters at breast height (DBH) were defined as ≥7.3 cm in Alberta and ≥9.7 cm in Saskatchewan, respectively, were marked and their DBH values were measured using DBH tapes (169 plots were removed); (d) each plot had at least 30 trees at initial measurement to ensure that the plot represented the sample forest, which resulted in the exclusion of plots with sizes <0.06 ha. In total, 871 plots were retained for analysis. Since the two provinces used different tree size criteria for monitoring, we selected trees with DBH ≥ 10 cm to standardize tree size difference sampled between the two provinces.

The mean for first census year was 1970, ranging from 1958 to 1993 (Supporting Information Figure S1). The mean for last census year was 1996, ranging from 1972 to 2009 (Supporting Information Figure S1). The measurement interval varied from 1 to 29 years, with a mean of 9.20 years. The number of censuses ranged from 3 to 8 times, with a mean of 3.9 times. A total of 3,415 censuses were taken, with 208,961 trees were measured during the monitoring period. Major species, which made up ≥1% of the total tree biomass across all plots and censuses, included *Populus tremuloides* (30.9), *Picea glauca* (30.8%) and *Pinus contorta* (23%), with minor of *Populus balsamifera* (5.8%), *Picea mariana* (3.2%), *Abies balsamea* (2.6%), *Pinus banksiana* (2.5%) and *Betula papyrifera* (1.3%).

2.2 | Calculations of net biomass change (ΔAGB), growth and mortality

Similar to Chen et al. (2016), we estimated the above-ground biomass of individual trees using published Canadian species-specific, DBH-based equations for wood, bark, foliage and branches (Lambert, Ung, & Raulier, 2005). These equations were developed based on ≥207 trees per species with variable sizes from Canadian boreal forests. For less frequently occurring species, we used general equations for softwood or hardwood to estimate their biomass (Lambert et al., 2005).

We calculated the ΔAGB (Mg ha^{-1} $year^{-1}$) at the stand level as the difference of living above-ground biomass between two

successive censuses divided by census interval. Similar to previous studies (Brienen et al., 2015; Chen & Luo, 2015), we defined the above-ground biomass growth as the sum of the growth of surviving trees and in-growth by new recruitment trees between two successive censuses divided by census length in years. The mortality component was the sum of above-ground biomass loss from all trees that died between two successive censuses divided by census length in years. Therefore, ΔAGB was the difference between growth and mortality. Observed tree mortality resulted from endogenous processes such as competition and longevity (Luo & Chen, 2011) and biotic and abiotic stressors such as heat, droughts, diseases and insects (Chen et al., 2018; Hogg et al., 2017), but not from fire and logging since government agencies discontinued monitoring once a stand-replacing disturbance occurred.

Long census intervals may underestimate mortality and growth because of the growth of unrecorded trees that are both recruited

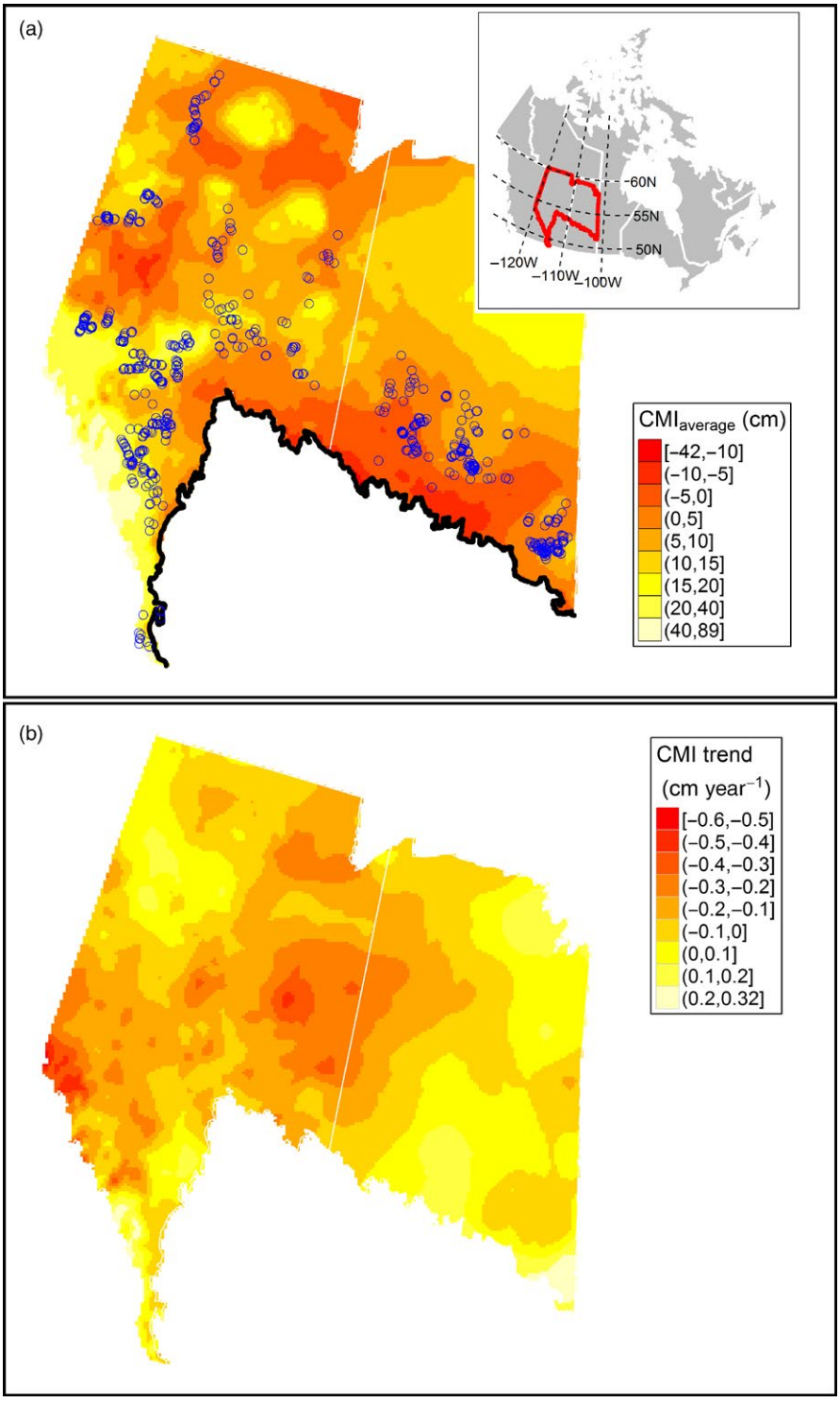

FIGURE 1 Plot locations and spatiotemporal patterns of annual climate moisture index between 1954 and 2011 in the study area. (a) Spatial climate moisture index defined as the long-term average of climate moisture index ($CMI_{average}$) between 1954 and 2011. (b) Temporal trend of annual climate moisture index (CMI) anomaly between 1954 and 2011. The study area is showed in the context of Canada. Blue open circles represent plot locations. The heavy black line is the border between boreal and prairie biomes [Colour figure can be viewed at wileyonlinelibrary.com]

and die during the interval (Brienen et al., 2015; Lewis et al., 2004). Following Chen et al. (2016), to correct for the unobserved recruits, we assumed that these occurred when trees were of smaller size (i.e., DBH between 10 and 15 cm). We estimated the number of unobserved recruits (U_r) as the number of stems in the plot (N) multiplied by the annual recruitment rate (R) multiplied by the mean annual mortality rate (M) multiplied by the census interval length (L): $U_r = N \times R \times M \times L$. To correct for unobserved growth and mortality related to trees that died within a census interval, we assumed that all such trees died at the midpoint, and assigned growth up to this midpoint, and estimated the median growth of all plot trees within the 10–15 cm DBH size class. The biomass associated with unobserved recruits accounted for, on average, 0.98% and 0.6% of the total growth and mortality, respectively, and thus will have a negligible effect on our analysis of growth and mortality.

2.3 | Stand age determination

Stand age (SA) for each plot was determined according to a known fire (that cleared the previous forest) or by coring at least three dominant/co-dominant trees of each tree species inside or outside the plot at the time of plot establishment. If coring was the method of forest age determination, the average ring counts for the species with the oldest ages were used to estimate time since fire, following species-specific relationships between forest age and time since fire developed for the boreal forests (Gutsell & Johnson, 2002; Vasiliauskas & Chen, 2002). Among the 871 selected plots, we determined stand ages of 176 by known fires, 695 from coring. Of these 695 plots, a total of 4,024 trees were cored, which included 367 *Pinus banksiana*, 455 *Pinus contorta*, 819 *Populus tremuloides*, 28 *Betula papyrifera*, 112 *Populus balsamea*, 334 *Picea mariana*, 1763 *Picea glauca*, six *Pseudotsuga menziesii*, 134 *Abies balsamea* and 6 *Abies lasiocarpa*.

2.4 | Climate variables

We used the long-term average of climate moisture availability/index ($CMI_{average}$) as a proxy for spatial water availability for the study area. The $CMI_{average}$ was calculated for the years between 1954 and 2011, during which plot measurements were taken (Supporting Information Figure S1). Annual CMI was the sum of monthly values over 12-month periods from last 1 August to 31 July of the current year (Hogg, Brandt, & Michaelian, 2008). The monthly CMI was based on the quantity of monthly precipitation minus monthly potential evapotranspiration (PET), which was computed using a simplified form of the Penman-Monteith equation (Hogg, 1997). Smaller (or more negative) CMI values indicate drier conditions (Hogg et al., 2008). To explore the potential climate drivers that may contribute to temporal changes of ΔAGB, growth and mortality, we calculated climate anomalies. These anomalies were defined as the departure of means between two sequential measurements from the long-term climate means (Clark, Bell, Hersh, & Nichols, 2011). We calculated two sets of climate anomalies: mean annual temperature anomaly (ATA) and annual climate moisture index anomaly (ACMIA). We derived the annual temperature and CMI data from BioSIM 10 (Réginère, Saint-Amant, & Béchard, 2014), which generates historical climate data for specific locations based on latitude, longitude and elevation. We obtained the atmospheric CO_2 data from the Mauna Loa Earth System Research Laboratory in Hawaii (http://www.esrl.noaa.gov/gmd/ccgg/trends/co2_data_mlo.html).

2.5 | Statistical analysis

We used a multivariate mixed effect model to examine ΔAGB, growth and mortality as dependent variables (Model 1), as the variance of ΔAGB depended on the variance of growth and mortality. Since ΔAGB, growth and mortality are strongly dependent on stand age (SA, years) (Chen & Luo, 2015; Chen et al., 2016; Coomes, Holdaway, Kobe, Lines, & Allen, 2012; Foster et al., 2010; Ryan, Binkley, & Fownes, 1997), we used SA to account for the effects of endogenous processes associated with stand development on ΔAGB, growth and mortality. To examine whether long-term climate change associated trends in ΔAGB, growth and mortality, similar to previous studies (Brienen et al., 2015; Luo & Chen, 2013), we used the middle calendar year of a census interval (Year) to represent climate change drivers as a whole. We used $CMI_{average}$ to represent the long-term average of climate moisture availability of each sample plot. As a result, the model included main effects of SA, Year and $CMI_{average}$ and their two-way interactions (Equation 1). In the model, a significant interaction term between Year and $CMI_{average}$ indicates the temporal trends of ΔAGB, growth and mortality vary along a spatial water availability gradient.

$$\begin{aligned}(\Delta\text{AGB, growth, mortality})_{ijk} = {} & \beta_1 + \beta_2 \cdot \ln\text{SA}_{ijk} + \beta_3 \cdot \text{Year}_{ijk} + \beta_4 \cdot (\text{CMI}_{\text{average}})_{ijk} \\ & + \beta_5 \cdot \ln\text{SA}_{ijk} \times \text{Year}_{ijk} + \beta_6 \cdot \ln\text{SA}_{ijk} \\ & \times (\text{CMI}_{\text{average}})_{ijk} + \beta_7 \cdot \text{Year}_{ijk} \\ & \times (\text{CMI}_{\text{average}})_{ijk} + \pi_j + \epsilon_{k(ij)}\end{aligned} \quad (1)$$

where lnSA was log-transformed SA, which was the best curve to describe our dependent variables based on the preliminary analyses (Chen et al., 2016); i and j were the ith census period in jth plot; βs were the fixed effects to be estimated; π_j was the random plot effect; $\epsilon_{k(ij)}$ is sampling error. The model did not include the three-way interaction among predictors, as the preliminary analyses indicated nonsignificant effects for all the biomass components $p = 0.36$, 0.37 and 0.64) for ΔAGB, growth and mortality, respectively. In our dataset, there was a positive but weak collinearity existed between SA and Year ($r = 0.16$ or $r^2 = 0.027$). In this study, effects of SA and Year on ΔAGB and its components were modelled simultaneously, as our preliminary analyses suggested that assigning priority to SA would marginalize the Year effect and vice versa (Brown et al., 2011).

Similar to previous studies (Brienen et al., 2015; Phillips et al., 2009), we weighted observations by Plot size$^{0.5}$ × length (where Plot size was in ha and Length was the number of years between two consecutive censuses) to account for the sampling heterogeneity (i.e., different measurement lengths and plot sizes). Alternatively,

we also weighted observations by Plot size × length, and the results were qualitatively similar. For simplicity, we reported the results using Plot size$^{0.5}$ × length as weightings.

The multivariate mixed effect model was performed using the *nlme* package (Pinheiro, Bates, DebRoy, & Sarkar, 2016). For our dependent variables, the distribution of ΔAGB and mortality were left right-skewed and right-skewed, respectively (Figure S2c,d), potentially violating the parametric assumption of normal distribution. To assess the robustness of the fixed effects, we conducted a nonparametric, rank-based mixed effect model using the *rlme* package (Bilgic, Susmann, & McKean, 2018). The rank-based mixed effect model gave outputs similar to the multivariate mixed model, except for growth, which revealed an insignificant fixed effect for Year and $CMI_{average}$ (Table S2). Results from univariate mixed models were also consistent with those from the multivariate mixed model (Table S2). The estimated mean fixed effects from the multivariate mixed model were internally consistent, that is, the sum of coefficients from mortality and growth were equal to ΔAGB in the multivariate model, but not in the univariate or rank-based model. For example, the difference between overall change rate of ΔAGB and those of growth minus mortality was 0.0001 Mg ha^{-1} year^{-1} year^{-1} estimated by the multivariate mixed effect model, but the difference was 0.0026 Mg ha^{-1} year^{-1} year^{-1} and 0.0059 Mg ha^{-1} year^{-1} year^{-1} from the rank-based mixed effect model and the univariate mixed model, respectively. Given that the multivariate mixed model can address the dependencies of the fixed effects, and can reach the same conclusion, we reported the results from the multivariate mixed model. We also inspected whether using the species-specific allometric equations misled our conclusion. We calculated annual net stand basal area change (m^2 ha^{-1} year^{-1}) and its growth and mortality components. The model demonstrated similar results to the above-ground biomass model (comparing Supporting Information Figure S3 with Figures 2 and 3f). Therefore, we subsequently focused our analysis on the changes in above-ground biomass.

We examined the temporal trends of climate drivers, that is, CO_2, ATA and ACMIA, using linear mixed effect models. To investigate the sensitivities of ΔAGB, growth and mortality to the climate drivers along climate moisture availability gradient, we replaced Year term in Equation 1 with CO_2, ATA and ACMIA individually. The sensitivity of a biomass component to the climate driver was defined as the change of the biomass component with a unit change of climate variable (Wolkovich et al., 2012). In each of these models, we calculated the sensitivity of ΔAGB and its components to a specific climate change driver along spatial water availability as $\beta_3 + \beta_7 \times CMI_{average}$ (where β_3 and β_7 were the estimated coefficients for climate change driver and the interaction term between climate driver and $CMI_{average}$) (Chen et al., 2016). To graphically show spatiotemporal patterns of ΔAGB, growth and mortality, we mapped plot-level average predictions on a grid of

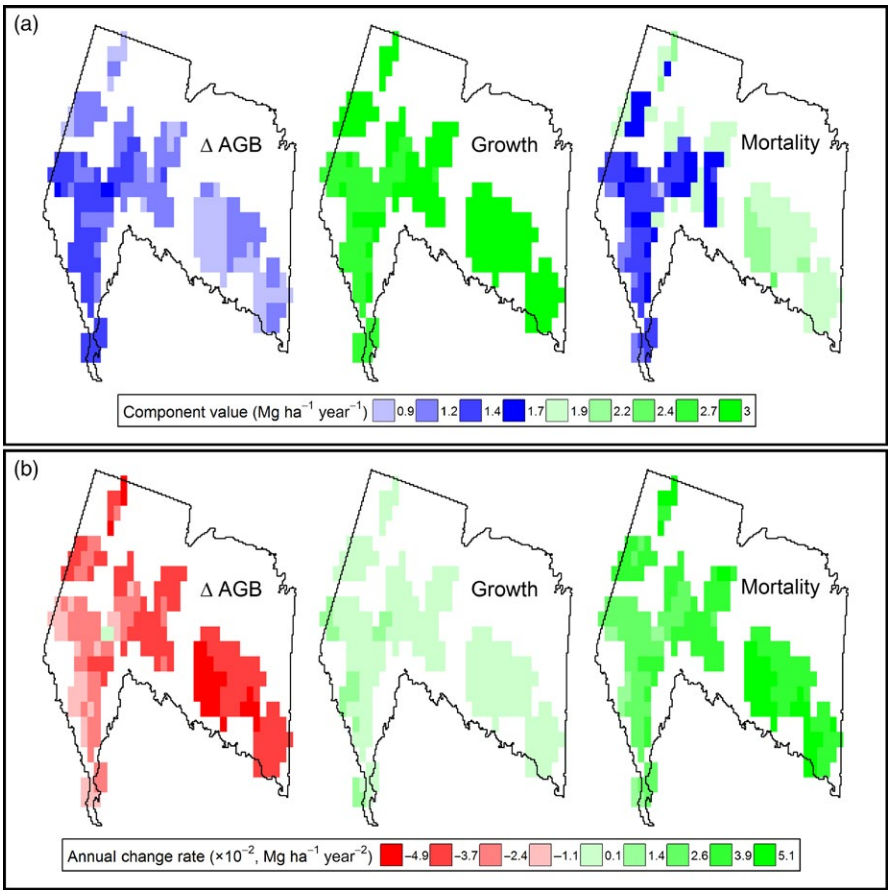

FIGURE 2 Predicted spatiotemporal patterns of net above-ground biomass change (ΔAGB), growth and mortality. (a) Long-term average ΔAGB, growth and mortality. (b) Temporal trends in ΔAGB, growth and mortality. The spatiotemporal patterns of ΔAGB, growth and mortality are summarized from the predictions for each plot using a multivariate mixed effect model that simultaneously accounts for stand age, year and $CMI_{average}$ effects (see Table 1 and Equation 1 in materials and methods). The value is averaged for each 0.5° in longitude by 0.5° in latitude grid [Colour figure can be viewed at wileyonlinelibrary.com]

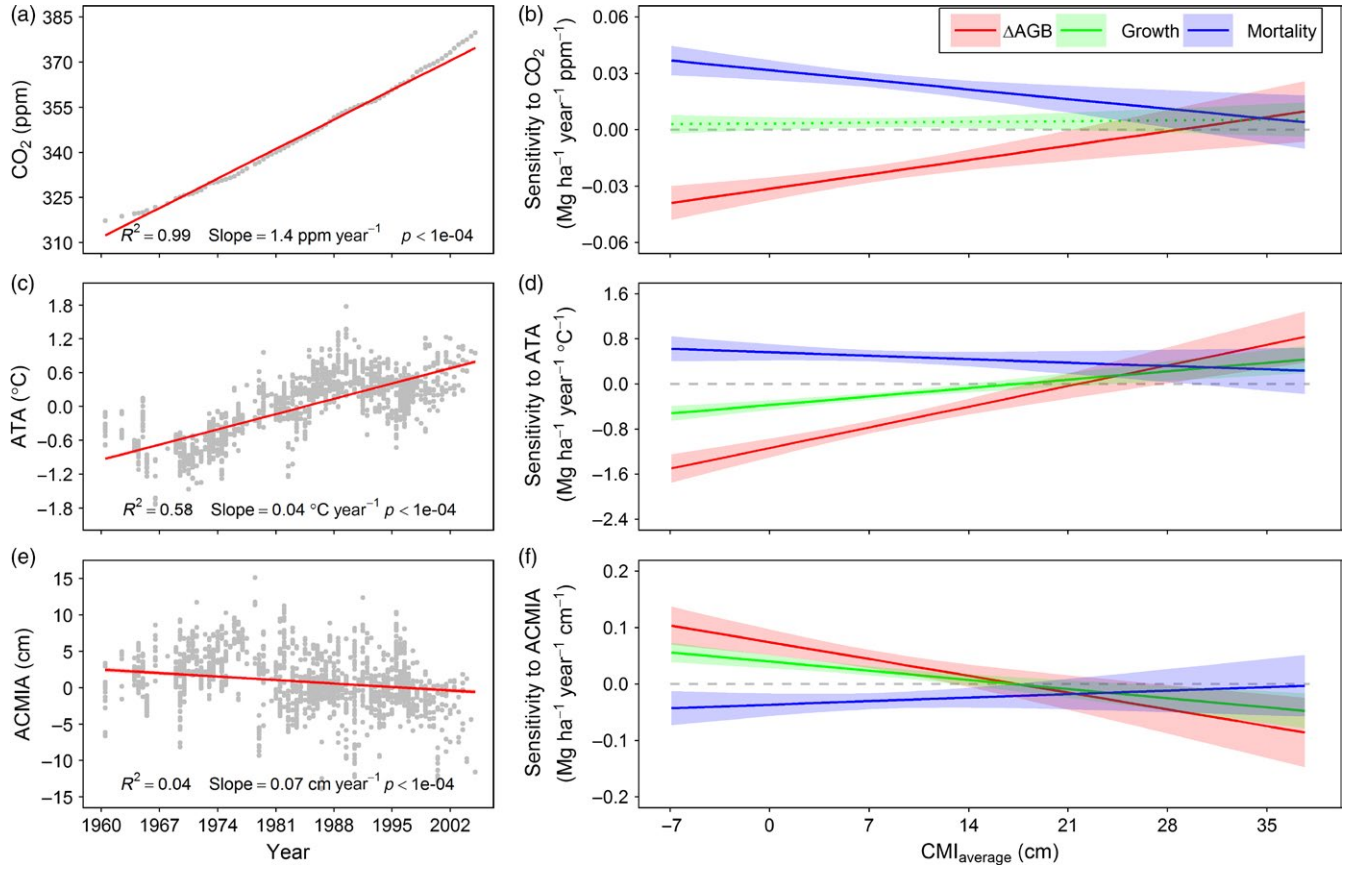

FIGURE 3 Temporal trends of climate drivers and the sensitivities of net above-ground biomass change (ΔAGB), growth and mortality to climate drivers along the gradient of the long-term average of climate moisture index ($CMI_{average}$). (a, c, e) Temporal changes in atmospheric CO_2 concentration (CO_2), mean annual temperature anomaly (ATA) and annual climate moisture index anomaly (ACMIA), respectively; grey dots are observed climates from the 871 plots; red line and shadow area are the fitted linear line and 95% confidence intervals in mixed effect model. (b, d and f) Sensitivities of ΔAGB, growth and mortality to the CO_2, ATA and ACMIA, respectively; lines and shadows are mean and 95 confidence interval summarized from multivariate mixed effect model that simultaneously takes account for stand age, climate driver and $CMI_{average}$ effects. The sensitivity is defined as the change of the biomass component per a unit change of climate (see materials and methods) [Colour figure can be viewed at wileyonlinelibrary.com]

0.5° in longitude by 0.5° in latitude. All the analyses were performed using R (R Development Core Team, 2017).

3 | RESULTS

Across all plots measured between 1958 and 2011, the average ΔAGB was 1.15 ± 0.05 (*M* ± *SEM*) Mg ha^{-1} year^{-1}. This positive average ΔAGB occurred as the result of higher above-ground biomass growth (2.89 ± 0.04 Mg ha^{-1} year^{-1}) than above-ground biomass loss from mortality (1.74 ± 0.05 Mg ha^{-1} year^{-1}) (Table 1). Our analyses showed that ΔAGB decreased with stand age and calendar year and increased with $CMI_{average}$ (Table 1). The age-related decline in net biomass change resulted from decreased growth and increased mortality associated with forest ageing. At the same time, ΔAGB decreased with the calendar year at 0.0314 Mg ha^{-1} year^{-2} due to substantially larger mortality loss (0.0368 Mg ha^{-1} year^{-2}) than growth gain (0.0053 Mg ha^{-1} year^{-2}) (Table 1). Mortality and growth decreased with $CMI_{average}$ by 0.04 and 0.01 Mg ha^{-1} year^{-1} cm^{-1}, respectively (Table 1). The weakening of mortality with increasing $CMI_{average}$ led to higher ΔAGB in moist sites than dry sites (Table 1; Figure 2a).

After controlling for stand age effects, ΔAGB decreased temporally on average at 0.031 ± 0.003 Mg ha^{-1} year^{-2}, driven primarily by a large mortality increase (0.037 ± 0.003 Mg ha^{-1} year^{-2}), accompanied by a small growth increase (0.005 ± 0.002 Mg ha^{-1} year^{-2}) (Table 1). Importantly, the temporal declines in ΔAGB were more prominent in drier conditions (positive Year × $CMI_{average}$ effect in Table 1, Figure 2b). The higher decline rate in drier conditions was primarily driven by increased mortality (Table 1).

The spatiotemporal response of ΔAGB, growth and mortality to $CMI_{average}$ may be related to variation in their sensitivities to recent climate change drivers. During the study period, global atmospheric CO_2 increased by 1.40 ppm year^{-1} (Figure 3a). For our study plots, annual temperature anomaly (ATA) increased by 0.04°C year^{-1} (Figure 3c); annual climate moisture index anomaly (ACMIA) decreased on average by 0.07 cm^{-1} year^{-1} (Figure 3e). Sensitivity analysis showed that ΔAGB responded to CO_2 in a similar way to Year because of the strong correlation between CO_2

TABLE 1 Fixed effects in year model using multivariate mixed effect model. For dependent variables, ΔAGB, growth and mortality are net above-ground biomass change, above-ground biomass growth and above-ground mortality, respectively. For predictors, lnSA, Year and $CMI_{average}$ are log-transformed stand age (years), calendar year and the long-term average of climate moisture index (cm) between 1954 and 2011, respectively

Variable	Predictor	Coefficient	*SEM*	*p*
ΔAGB	Intercept	1.1497	0.0502	<0.0001
	lnSA	−2.6846	0.1293	<0.0001
	Year	−0.0314	0.0031	<0.0001
	$CMI_{average}$	0.0257	0.0065	0.0001
	lnSA × Year	−0.0264	0.0080	0.0010
	lnSA × $CMI_{average}$	0.0021	0.0153	0.8931
	Year × $CMI_{average}$	0.0016	0.0004	<0.0001
Growth	Intercept	2.8891	0.0349	<0.0001
	lnSA	−1.5095	0.0890	<0.0001
	Year	0.0053	0.0018	0.0033
	$CMI_{average}$	−0.0135	0.0045	0.0029
	lnSA × Year	−0.0134	0.0045	0.0029
	lnSA × $CMI_{average}$	0.0159	0.0106	0.1327
	Year × $CMI_{average}$	0.0002	0.0002	0.2899
Mortality	Intercept	1.7394	0.0464	<0.0001
	lnSA	1.1766	0.1195	<0.0001
	Year	0.0368	0.0028	<0.0001
	$CMI_{average}$	−0.0392	0.0060	<0.0001
	lnSA × Year	0.0128	0.0072	0.0744
	lnSA × $CMI_{average}$	0.0139	0.0142	0.3286
	Year × $CMI_{average}$	−0.0014	0.0003	<0.0001

Note. *SEM*, standard error of mean.

and Year (Figure 3a). On average, ΔAGB decreased by 0.664 ± 0.0 56 Mg ha^{-1} $year^{-1}$ $°C^{-1}$ with ATA and increased by 0.045 ± 0.008 M g ha^{-1} $year^{-1}$ cm^{-1} with ACMIA (Supporting Information Table S3). The sensitivities of ΔAGB to these climate change drivers were, however, significantly dependent on $CMI_{average}$. ΔAGB was more sensitive climate change drivers at low $CMI_{average}$ (Figure 3b,d,f). Increasing CO_2 led to higher mortality, accompanied by no change in growth, at lower $CMI_{average}$ (Figure 3b). Increasing ATA resulted in less growth and more mortality at lower $CMI_{average}$ (Figure 3d). Decreasing ACMIA resulted in less growth and more mortality at lower $CMI_{average}$ (Figure 3f).

4 | DISCUSSION

Our study showed that after accounting for the effect of stand age, net above-ground biomass change of established forests on average increased with the long-term average of climate moisture availability of study plots, indicating that water availability constrained the capacity of the forests to accumulate biomass in our study area. The increase of net above-ground biomass change associated with increasing climate moisture availability was driven primarily by the declines in mortality, which was higher than the decreases in growth. The higher mortality in drier areas could be a result of long-term water deficit related to the hydraulic failure, carbon starvation and forest pests, or combinations thereof (Allen et al., 2015; Anderegg et al., 2015; Meir, Mencuccini, & Dewar, 2015; Rowland et al., 2015). As for the higher growth in drier areas, the underlying mechanisms are unclear, and it could be attributable to a species compositional change (Chen & Luo, 2015). In our study area, *Populus* spp. and *Pinus* spp., which may have high growth rates, tend to colonize the drier areas, whereas slow-growing *Picea* spp. are frequently distributed in moist areas (Burns & Honkala, 1990). Alternatively, the variation in growth along the climate moisture gradient may be attributable to reduced competition because of higher mortality (Luo & Chen, 2015).

Consistent with previous studies (Chen & Luo, 2015; Chen et al., 2016; Ma et al., 2012), we found that net biomass change decreased temporally on average across all study plots during the study period, resulting from increased mortality with slightly increased growth. Importantly, we found that the temporal trends in net above-ground biomass change varied spatially along the gradient of the long-term average of climate moisture availability, with a pronounced temporal decrease in the dry plots, due to a stronger temporal increase in mortality than an increase in growth. Our results indicated that although rising CO_2, warming and associated increases in growing season length could increase tree growth in boreal forests (Girardin, Bouriaud, et al., 2016; Pretzsch et al., 2014), these positive climate change drivers for growth could be constrained by limited water availability (Chen et al., 2018; Hogg et al., 2017; Wang et al., 2014).

Our sensitivity analysis showed that net biomass change, growth and mortality responded to rising atmospheric CO_2

similarly to the overall temporal trends observed through the calendar year. While increased growth associated with rising atmospheric CO_2 is attributable to the effects of CO_2 fertilization (Brienen et al., 2015; Huang, Bergeron, Denneler, Berninger, & Tardif, 2007; Pretzsch et al., 2014), increased tree mortality associated with rising atmospheric CO_2 could have resulted from increased competition (Luo & Chen, 2015) and reduced tree longevity (Brienen et al., 2015). In dry plots, warming had strong negative effects on net biomass change due to increased mortality and reduced growth. These negative effects of warming could reflect the coupling influences of direct heat stress and increased activity of insects (Allen et al., 2015; Anderegg et al., 2015; Chen et al., 2018; Hogg et al., 2017). With temporally decreasing climate moisture availability, which resulted from temporally increasing PET despite slightly increasing precipitation in the study area (Luo & Chen, 2013), net biomass change decreased in dry plots, due to a decrease in growth and an increase in mortality. However, net biomass change in wet plots was substantially less sensitive to temporal increases in temperature and decreases in climate moisture availability. These results further confirm that climate change-induced growth and mortality dynamics are profoundly influenced by the long-term average of climate moisture availability, with more water buffering the effects of heat stress and warming-induced water deficits (Peng et al., 2011; Searle & Chen, 2017).

Given that the future climate projections show decreasing water availability for most terrestrial ecosystems, coupled with an increase of temperature (IPCC, 2013), our results have three significant implications. First, projections of future climate change-related variations in forest carbon cycling should consider the divergent responses of above-ground biomass change along with climate moisture gradients. For example, our results showing above-ground biomass change is declining most rapidly in dry areas suggest that forests in dry areas may soon become a carbon source if climate trends continue, even without increasing stand-replacing disturbances. Second, our results suggest that climate changes may lead to an abrupt retreat of the boreal biome in our study area at the trailing edge (Gladwell, 2006; Scheffer, Hirota, Holmgren, Van Nes, & Chapin, 2012). For example, forests at the drier distribution limits such as the boreal-prairie ecotone (Figure 1) consist of less biomass and are more vulnerable to its loss due to climate changes than the forests at the core of our study area (i.e., central boreal forest). This study and previous studies conducted at leading edge (Beck et al., 2011; McManus et al., 2012) are consistent with the projected boreal biome shift northward under climate changes (Parmesan & Yohe, 2003). Lastly, given that both mortality and growth shape spatiotemporal patterns of net above-ground biomass change, simultaneous assessment of their dynamics will be required to make any inferences regarding the response of forest communities to climate changes.

ACKNOWLEDGEMENTS

We thank the Forest Management Branch of Alberta Ministry of Sustainable Resource Development and the Forestry Branch of Saskatchewan for providing detailed data. This study was supported by the Natural Sciences and Engineering Research Council of Canada (RGPIN-2014-04181 and STPGP 506284).

AUTHORS' CONTRIBUTIONS

Y.L. and H.Y.H.C. designed the study; Y.L. compiled the data; Y.L., H.Y.H.C. and E.J.B.M. analysed the data; Y.L., H.Y.H.C., E.J.B.M. and D.W.A. wrote the paper.

DATA ACCESSIBILITY

Data available from the Dryad Digital Repository: https://doi.org/10.5061/dryad.8bg44b0 (Luo, Chen, McIntire, & Andison, 2018).

ORCID

Han Y. H. Chen http://orcid.org/0000-0001-9477-5541

REFERENCES

Allen, C. D., Breshears, D. D., & McDowell, N. G. (2015). On underestimation of global vulnerability to tree mortality and forest die-off from hotter drought in the Anthropocene. *Ecosphere*, *6*, 1–55.

Anderegg, W. R., Hicke, J. A., Fisher, R. A., Allen, C. D., Aukema, J., Bentz, B., … Zeppel, M. (2015). Tree mortality from drought, insects, and their interactions in a changing climate. *New Phytologist*, *208*, 674–683. https://doi.org/10.1111/nph.13477

Beck, P. S., Juday, G. P., Alix, C., Barber, V. A., Winslow, S. E., Sousa, E. E., … Goetz, S. J. (2011). Changes in forest productivity across Alaska consistent with biome shift. *Ecology Letters*, *14*, 373–379. https://doi.org/10.1111/j.1461-0248.2011.01598.x

Bilgic, Y., Susmann, H., & McKean, J. (2018). *rlme: Rank-based estimation and prediction in random effects nested models*. R package version, 5.

Bloom, A. J., Chapin, F. S., & Mooney, H. A. (1985). Resource limitation in plants-an economic analogy. *Annual Review of Ecology and Systematics*, *16*, 363–392. https://doi.org/10.1146/annurev.es.16.110185.002051

Bradshaw, C. J. A., & Warkentin, I. G. (2015). Global estimates of boreal forest carbon stocks and flux. *Global and Planetary Change*, *128*, 24–30. https://doi.org/10.1016/j.gloplacha.2015.02.004

Brienen, R. J., Phillips, O. L., Feldpausch, T. R., Gloor, E., Baker, T. R., Lloyd, J., … Zagt, R. J. (2015). Long-term decline of the Amazon carbon sink. *Nature*, *519*, 344–348. https://doi.org/10.1038/nature14283

Brown, C. J., Schoeman, D. S., Sydeman, W. J., Brander, K., Buckley, L. B., Burrows, M., … Richardson, A. J. (2011). Quantitative approaches in climate change ecology. *Global Change Biology*, *17*, 3697–3713. https://doi.org/10.1111/j.1365-2486.2011.02531.x

Burns, R. M., & Honkala, B. H. (1990). *Silvics of North America*. Washington, DC: U.S. Department of Agriculture, Forest Service.

Chen, L., Huang, J. G., Dawson, A., Zhai, L., Stadt, K. J., Comeau, P. G., & Whitehouse, C. (2018). Contributions of insects and droughts to growth decline of trembling aspen mixed boreal forest of western Canada. *Global Change Biology*, *24*, 655–667. https://doi.org/10.1111/gcb.13855

Chen, H. Y. H., & Luo, Y. (2015). Net aboveground biomass declines of four major forest types with forest ageing and climate change in western Canada's boreal forests. *Global Change Biology*, *21*, 3675–3684. https://doi.org/10.1111/gcb.12994

Chen, H. Y. H., Luo, Y., Reich, P. B., Searle, E. B., & Biswas, S. R. (2016). Climate change-associated trends in net biomass change are age dependent in western boreal forests of Canada. *Ecology Letters*, *19*, 1150–1158. https://doi.org/10.1111/ele.12653

Clark, J. S., Bell, D. M., Hersh, M. H., & Nichols, L. (2011). Climate change vulnerability of forest biodiversity: Climate and competition tracking of demographic rates. *Global Change Biology*, *17*, 1834–1849. https://doi.org/10.1111/j.1365-2486.2010.02380.x

Coomes, D. A., Holdaway, R. J., Kobe, R. K., Lines, E. R., & Allen, R. B. (2012). A general integrative framework for modelling woody biomass production and carbon sequestration rates in forests. *Journal of Ecology*, *100*, 42–64. https://doi.org/10.1111/j.1365-2745.2011.01920.x

Dai, A. (2013). Increasing drought under global warming in observations and models. *Nature Climate Change*, *3*, 52–58. https://doi.org/10.1038/nclimate1633

Dixon, R. K., Solomon, A. M., Brown, S., Houghton, R. A., Trexier, M. C., & Wisniewski, J. (1994). Carbon pools and flux of global forest ecosystems. *Science*, *263*, 185–190. https://doi.org/10.1126/science.263.5144.185

D'Orangeville, L., Duchesne, L., Houle, D., Kneeshaw, D., Côté, B., & Pederson, N. (2016). Northeastern North America as a potential refugium for boreal forests in a warming climate. *Science*, *352*, 1452–1455. https://doi.org/10.1126/science.aaf4951

Food and Agriculture Organization of the United Nations (2015). *Global forest resources assessment 2015 – How are the world's forests changing?* Rome, Italy: Food and Agriculture Organization of the United Nations.

Foster, J. R., Burton, J. I., Forrester, J. A., Liu, F., Muss, J. D., Sabatini, F. M., … Mladenoff, D. J. (2010). Evidence for a recent increase in forest growth is questionable. *Proceedings of the National Academy of Sciences of the United States of America*, *107*, E86–E87. https://doi.org/10.1073/pnas.1002725107

Girardin, M. P., Bouriaud, O., Hogg, E. H., Kurz, W., Zimmermann, N. E., Metsaranta, J. M., … Bhatti, J. (2016). No growth stimulation of Canada's boreal forest under half-century of combined warming and CO2 fertilization. *Proceedings of the National Academy of Sciences of the United States of America*, *113*, E8406–E8414. https://doi.org/10.1073/pnas.1610156113

Girardin, M. P., Hogg, E. H., Bernier, P. Y., Kurz, W. A., Guo, X. J., & Cyr, G. (2016). Negative impacts of high temperatures on growth of black spruce forests intensify with the anticipated climate warming. *Global Change Biology*, *22*, 627–643. https://doi.org/10.1111/gcb.13072

Gladwell, M. (2006). *The tipping point: How little things can make a big difference*. Boston, MA: Little, Brown.

Gutsell, S. L., & Johnson, E. A. (2002). Accurately ageing trees and examining their height-growth rates: Implications for interpreting forest dynamics. *Journal of Ecology*, *90*, 153–166. https://doi.org/10.1046/j.0022-0477.2001.00646.x

Hogg, E. H. (1997). Temporal scaling of moisture and the forest-grassland boundary in western Canada. *Agricultural and Forest Meteorology*, *84*, 115–122. https://doi.org/10.1016/S0168-1923(96)02380-5

Hogg, E. H., Brandt, J. P., & Michaelian, M. (2008). Impacts of a regional drought on the productivity, dieback, and biomass of western Canadian aspen forests. *Canadian Journal of Forest Research*, *38*, 1373–1384. https://doi.org/10.1139/X08-001

Hogg, E. H., Michaelian, M., Hook, T. I., & Undershultz, M. E. (2017). Recent climatic drying leads to age-independent growth reductions of white spruce stands in western Canada. *Global Change Biology*, *23*, 5297–5308. https://doi.org/10.1111/gcb.13795

Huang, J. G., Bergeron, Y., Denneler, B., Berninger, F., & Tardif, J. (2007). Response of forest trees to increased atmospheric CO2. *Critical Reviews in Plant Sciences*, *26*, 265–283. https://doi.org/10.1080/07352680701626978

IPCC (2013). *Climate change 2013 – The physical science basis*. New York, NY: Cambridge University Press.

Lambert, M. C., Ung, C. H., & Raulier, F. (2005). Canadian national tree aboveground biomass equations. *Canadian Journal of Forest Research-Revue Canadienne De Recherche Forestiere*, *35*, 1996–2018. https://doi.org/10.1139/x05-112

Larsen, C. P. S. (1997). Spatial and temporal variations in boreal forest fire frequency in northern Alberta. *Journal of Biogeography*, *24*, 663–673. https://doi.org/10.1111/j.1365-2699.1997.tb00076.x

Lewis, S. L., Phillips, O. L., Sheil, D., Vinceti, B., Baker, T. R., Brown, S., … Martinez, R. V. (2004). Tropical forest tree mortality, recruitment and turnover rates: Calculation, interpretation and comparison when census intervals vary. *Journal of Ecology*, *92*, 929–944. https://doi.org/10.1111/j.0022-0477.2004.00923.x

Liu, Y. Y., van Dijk, A. I. J. M., de Jeu, R. A. M., Canadell, J. G., McCabe, M. F., Evans, J. P., & Wang, G. (2015). Recent reversal in loss of global terrestrial biomass. *Nature Climate Change*, *5*, 470–474. https://doi.org/10.1038/nclimate2581

Luo, Y., & Chen, H. Y. H. (2011). Competition, species interaction and ageing control tree mortality in boreal forests. *Journal of Ecology*, *99*, 1470–1480. https://doi.org/10.1111/j.1365-2745.2011.01882.x

Luo, Y., & Chen, H. Y. H. (2013). Observations from old forests underestimate climate change effects on tree mortality. *Nature Communications*, *4*, 1965.

Luo, Y., & Chen, H. Y. H. (2015). Climate change-associated tree mortality increases without decreasing water availability. *Ecology Letters*, *18*, 1207–1215. https://doi.org/10.1111/ele.12500

Luo, Y., Chen, H. Y. H., McIntire, E. J. B., & Andison, D. W. (2018). Data from: Divergent temporal trends of net biomass change in western Canadian boreal forests. *Dryad Digital Repository*, https://doi.org/10.5061/dryad.8bg44b0

Ma, Z., Peng, C., Zhu, Q., Chen, H., Yu, G., Li, W., … Zhang, W. (2012). Regional drought-induced reduction in the biomass carbon sink of Canada's boreal forests. *Proceedings of the National Academy of Sciences of the United States of America*, *109*, 2423–2427. https://doi.org/10.1073/pnas.1111576109

McManus, K. M., Morton, D. C., Masek, J. G., Wang, D., Sexton, J. O., Nagol, J. R., … Boudreau, S. (2012). Satellite-based evidence for shrub and graminoid tundra expansion in northern Quebec from 1986 to 2010. *Global Change Biology*, *18*, 2313–2323. https://doi.org/10.1111/j.1365-2486.2012.02708.x

Meir, P., Mencuccini, M., & Dewar, R. C. (2015). Drought-related tree mortality: Addressing the gaps in understanding and prediction. *New Phytologist*, *207*, 28–33. https://doi.org/10.1111/nph.13382

Pan, Y., Birdsey, R. A., Fang, J., Houghton, R., Kauppi, P. E., Kurz, W. A., … Hayes, D. (2011). A large and persistent carbon sink in the world's forests. *Science*, *333*, 988–993. https://doi.org/10.1126/science.1201609

Parmesan, C., & Yohe, G. (2003). A globally coherent fingerprint of climate change impacts across natural systems. *Nature*, *421*, 37–42. https://doi.org/10.1038/nature01286

Peng, C. H., Ma, Z. H., Lei, X. D., Zhu, Q., Chen, H., Wang, W. F., … Zhou, X. L. (2011). A drought-induced pervasive increase in tree mortality across Canada's boreal forests. *Nature Climate Change*, *1*, 467–471. https://doi.org/10.1038/nclimate1293

Phillips, O. L., Aragao, L. E., Lewis, S. L., Fisher, J. B., Lloyd, J., Lopez-Gonzalez, G., … Torres-Lezama, A. (2009). Drought sensitivity of the Amazon rainforest. *Science*, *323*, 1344–1347. https://doi.org/10.1126/science.1164033

Pinheiro, J., Bates, D., DebRoy, S., & Sarkar, D. & R Core Team. (2016). *nlme: Linear and nonlinear mixed effects models*. R package version 3.1-127.

Pretzsch, H., Biber, P., Schutze, G., Uhl, E., & Rotzer, T. (2014). Forest stand growth dynamics in Central Europe have accelerated since 1870. *Nature Communications*, *5*, 4967. https://doi.org/10.1038/ncomms5967

R Development Core Team. (2017). *R: A Language and Environment for Statistical Computing*. *Version 3.4.2*. Vienna, Austria: R Foundation for Statistical Computing.

Réginère, J., Saint-Amant, R., & Béchard, A. (2014). *BioSIM 10 user's manual*. *Information Report LAU-X-137E*. Sainte-Foy, QC: Natural Resources Canada.

Rowland, L., da Costa, A. C. L., Galbraith, D. R., Oliveira, R. S., Binks, O. J., Oliveira, A. A. R., … Meir, P. (2015). Death from drought in tropical forests is triggered by hydraulics not carbon starvation. *Nature*, *528*, 119–122.

Ryan, M. G., Binkley, D., & Fownes, J. H. (1997). Age-related decline in forest productivity: Pattern and process. In M. Begon, & A. H. Fitter (Eds.), *Advances in ecological research* (pp. 213–262). London, UK: Academic Press Ltd-Elsevier Science Ltd.

Scheffer, M., Hirota, M., Holmgren, M., Van Nes, E. H., & Chapin, F. S. 3rd (2012). Thresholds for boreal biome transitions. *Proceedings of the National Academy of Sciences of the United States of America*, *109*, 21384–21389. https://doi.org/10.1073/pnas.1219844110

Searle, E. B., & Chen, H. Y. H. (2017). Climate change-associated trends in biomass dynamics are consistent across soil drainage classes in western boreal forests of Canada. *Forest Ecosystems*, *4*, https://doi.org/10.1186/s40663-40017-40106-y

Vasiliauskas, S. A., & Chen, H. Y. H. (2002). How long do trees take to reach breast height after fire in northeastern Ontario? *Canadian Journal of Forest Research*, *32*, 1889–1992. https://doi.org/10.1139/x02-104

Wang, X., Piao, S., Ciais, P., Friedlingstein, P., Myneni, R. B., Cox, P., … Chen, A. (2014). A two-fold increase of carbon cycle sensitivity to tropical temperature variations. *Nature*, *506*, 212–215. https://doi.org/10.1038/nature12915

Weir, J. M. H., Johnson, E. A., & Miyanishi, K. (2000). Fire frequency and the spatial age mosaic of the mixed-wood boreal forest in western Canada. *Ecological Applications*, *10*, 1162–1177. https://doi.org/10.1890/1051-0761(2000)010[1162:FFATSA]2.0.CO;2

Wolkovich, E. M., Cook, B. I., Allen, J. M., Crimmins, T. M., Betancourt, J. L., Travers, S. E., … Cleland, E. E. (2012). Warming experiments underpredict plant phenological responses to climate change. *Nature*, *485*, 494–497. https://doi.org/10.1038/nature11014

SUPPORTING INFORMATION

Additional supporting information may be found online in the Supporting Information section at the end of the article.

How to cite this article: Luo Y, Chen HYH, McIntire EJB, Andison DW. Divergent temporal trends of net biomass change in western Canadian boreal forests. *J Ecol*. 2019;107:69–78. https://doi.org/10.1111/1365-2745.13033